https://doi.org/10.15407/ufm.23.04.658

M.A. LATYPOVA[1,*], S.L. KUZMIN[2,], T.D. FEDOROVA[2], and D.N. LAWRINUK[2]**

[1] Karaganda Industrial University,
Republic Ave., 30; 101400 Temirtau, Kazakhstan
[2] Rudny Industrial Institute,
50 Let Oktyabrya Str., 38; 111500 Rudny, Kazakhstan
* m.latypova@tttu.edu.kz, ** info@rii.kz

LOCALIZATION OF DEFORMATION IN THE PROCESS OF LARGE PLASTIC DEFORMATIONS

Experimental studies show that localization of plastic flow occurs both in quasi-static and dynamic deformations of metals. It leads to the formation of selected areas (lines, shear bands), in which the magnitude of plastic deformation and the density of crystal-lattice defects (dislocations) are several times higher than the values of these elements in the surrounding metal. Localization is a manifestation of the instability of plastic deformation, a consequence of fact that in such areas of localized flow, for one reason or another one, plastic deformation proceeds more easily than in the surrounding material. The formation of localization areas reduces the shear strength of metals; so, this effect should be taken into account when modelling elastoplastic deformation of metals. In addition, the formation of areas with a high density of defects can initiate a change in the internal structure of the metal, *e.g.*, the formation of new grain boundaries during intense plastic deformation. Therefore, the study of the mechanisms and conditions of localization of plastic flow is an urgent task of deformable-solid mechanics and is important both for numerical modelling of elastoplastic flows in metals and from the point of view of forecasting the structure and mechanical properties of deformed metal. Localization of plastic flow at the low and moderate strain rates has been studied in detail in a number of works. At the same time, there is no common understanding of the mechanisms and specific features of the localization of plastic flow.

Keywords: plastic deformation, plastic flow, microstructure, mechanical properties, martensite.

Citation: M.A. Latypova, S.L. Kuzmin, T.D. Fedorova, and D.N. Lawrinuk, Localization of Deformation in the Process of Large Plastic Deformations, *Progress in Physics of Metals*, **23**, No. 4: 658–683 (2022)

1. Introduction

Currently, it is generally recognized that plastic deformation develops heterogeneously in time and volume of the material. It has been experimentally established [1] that macrolocation of plastic flow takes place at all stages of plastic flow, and not only at the stage of macroscopic neck formation, as traditionally thought. At the same time, the number of actually existing forms of such localization is limited, and the appearance of any of them is uniquely determined by the regime of plastic flow and the law of deformation hardening acting throughout the appropriate stage of the deformation process [2, 3].

In this paper [4], the regularities of the development of localization of plastic deformation at the parabolic stage of plastic flow and the stage of pre-destruction of zirconium alloy under uniaxial stretching states are examined when instabilities of plastic deformation occur with a subsequent transition to the formation of a macroscopic neck. According to the prevailing ideas, the developed plastic deformation always occurs inhomogeneously, which is due to the alternation of hardening and relaxation processes in local volumes of the material. Interconnected collective effects at the meso- and macroscale levels can result in the establishment of an oscillatory regime characterized by periodic changes in the defective structure and mechanical properties of materials.

Studies of the processes of localization and instability of plastic flow, carried out in Refs. [5, 6], allowed us to fix the cyclic nature of the spatial-temporal process of evolution of local strain distributions, accompanied by the emergence of an oscillatory process in the material of the type 'hardening–softening'. This process, according to Ref. [6], causes the periodic formation of regions of locally softened material in the sample, namely, 'running necks', long before the appearance of a stable neck and subsequent destruction.

Despite the available information about the pulsating nature of the development of the localization of flow with large plastic deformations and attempts to explain them, including in the framework of synergetic models [7], the physical causes of instability at the final stage of the plastic flow remain unclear. This is due to the fact that not all details of macrolocalization with large plastic deformations have been studied equally due to methodological difficulties encountered in the study of deformations in locally deformed regions of the sample directly during the flow.

Nevertheless, knowledge of the patterns of occurrence and development of the deformation localization, leading to the loss of stability of plastic flow and destruction when changing shape, is of great practical importance, particularly, for assessing the reserve of technological plasticity of zirconium alloys subjected to large deformations in the process of obtaining finished products [8].

2. Features of the Localization of Deformation

Macroscopic deformation of metals is homogeneous over a limited range of loading parameters. With a decrease in temperature, an increase in the deformation rate, or a decrease in the grain size of the material, various inhomogeneities of the plastic flow are observed manifested in the formation of areas of localization of plastic deformation where its values can reach several tens. A large number of works from the last 50 years have been devoted to the study of the localization phenomenon [9, 10]. The inhomogeneity of high-speed plastic deformation, manifested in the formation of narrow shear planes, is known as adiabatically sheared bands. These are two-dimensional, almost flat formations in which the two sides of the region are displaced relative to each other, like cracks of the 2nd or 3rd type, but the material remains physically continuous. The characteristics of the shear bands depend significantly on the parameters of the loading process. The width of the bands is usually from a dozen to several hundred micrometres, while the length of the bands can be several millimetres or even centimetres. The observed aspect ratios reach values of hundreds or even thousands of units. Up to 90% of all plastic deformation of the material is concentrated in the shear bands; large shear deformations are also observed in the immediate vicinity of the shear bands [11]. The shear bands have a complex structure of highly deformed material and contain structures of dislocations and nanocrystalline grains [12] (Fig. 1).

Since ancient times, shear bands have been observed in metallurgical processes and were first described in Ref. [13]. In early works, they were often referred to as 'thermal stripes' [14] or white etching borders [15]. Subsequently, it became clear [16] that there are different types of shear bands that differ from each other in their internal structure. The bands observed in alloys are particularly distinguished, where the heating of the material leads to another important practical example, where localization is clearly visible and has been observed for a long time, is the process of punching metal barriers with a solid metal striker. In the first works [17], it was suggested that the formation of shear bands during the deformation of the striker is an undesirable process that should be eliminated. However, later [18], it was shown that it is the formation of shear bands that allows the striker to penetrate deeper into the material by reducing the diameter of its front end and, consequently, reducing the resistance to its movement. This idea of 'self-forming' drummers was supported in Refs. [19, 20].

In many early works, when stating the fact of formation of shear bands, there is no discussion of the causes of their origin. The first important step in this direction belongs to the work [15]. Authors [15] suggested that a local increase in temperature during deformation leads

to softening of the material; it is the competition of the mechanisms of thermal softening and deformation hardening, which leads to instability of the plastic flow and localization of plastic deformation. This point of view was supported by many authors and, until recently, was often perceived as the only possible one. At the same time, for a large number of materials, which manifest the localization of plastic deformation, an insignificant increase in temperature occurs during deformation, which, apparently, is not enough for significant softening of a uniformly deformable material [21]. The causes and mechanisms of the formation of localization bands, despite a huge number of studies of the phenomenon itself, remain controversial. There are several approaches to this problem, which differ from each other by the main mechanism, which is proposed by the authors as the main reason for the formation of areas of local softening against the background of uniform deformation hardening of the surrounding material.

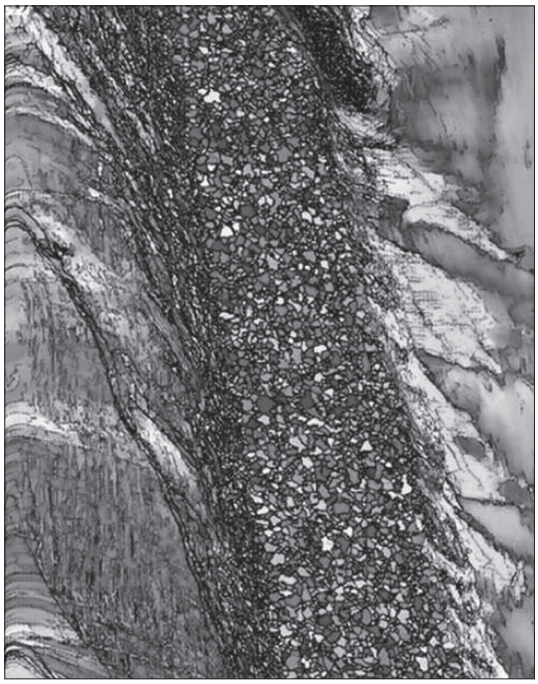

Fig. 1. Grinding of the grain structure inside the shear band [12]

In most metallic materials, including austenitic steels, with large degrees of deformation, there is a transition from homogeneous deformation to localization of deformation at various scale levels. At the same time, areas of intense plastic flow arise in the material, which at the microlevel represent localized shear bands or deformation localization bands, *i.e.*, shear bands. In this section, the main attention is paid to shear bands, as the most characteristic defective structures of austenitic steels are formed under states of large plastic deformations. Significant shear deformation is localized in these bands, and a wide range of disorientations of the crystal lattice and nanostructural states are formed.

When considering deformation localization bands of the type of shear bands, two types of bands are distinguished. The first type develops in a lamellar structure composed of twin/matrix layers [22–24], and bands of this type are characteristic of many f.c.c. metals with low ($\leq$20 mJ/m^2)

and medium (20–40 mJ/m^2) packing defect energy (PDE), as well as materials with high (40 mJ/m^2 or more) PDE under specific states of low temperatures and high deformation rates, such as Cu, Cu–Al, and Cu–Zn under states of dynamic (high-speed) plastic deformation, deformation with cooling in liquid nitrogen [25–27]. Under these states, even in f.c.c. metals with high PDE, intensive twinning is realized with the formation of double/matrix land structures. Under normal deformation states, metals with low PDE are deformed mainly by twinning, with low and medium PDE, by twinning and sliding, and with high PDE, by sliding.

In a microstrip structure, the second type of deformation localization bands forms from dislocation formations with small-angle boundaries: double dense dislocation walls (DDW) and low-energy dislocation substructures (LEDS) [28]. These bands are formed in many materials with high PDE (Cu, Al, and Ni) under deformation states at room temperature [29–32], in austenitic steels under deformation states at high temperatures [33] and in steels of other classes: ferritic, martensitic, *etc.* [34].

In addition to the two types of shear bands presented above, adiabatic shear bands (ASB), the most studied to date, should be noted [35–37]. These bands are distinguished by their formation states, which include high-speed loading, ~ 10^3–10^6 s^{-1} (shock loads), and adiabatic deformation. At the same time, in addition to large degrees and high deformation rates, the achieved high temperatures, high heating and cooling rates have a significant impact.

To date, the features of the microstructure and mechanisms of formation of the first type of shear bands in copper and copper alloys under dynamic plastic deformation (DPD) at cryogenic temperatures have been studied in the most detail [38–40]. The formation states and microstructure features of these strips are in many ways similar to those in austenitic steels.

The formation of localization bands is a characteristic feature of the deformation structure of austenitic steels after medium (e = 0.7–1.2, where e is a true deformation) degrees of deformation [41]. It is established that their main feature is the presence of significant shear deformation (γ = 1–10). Shear bands are plastic-like regions of the material within which the shifts are concentrated, parallel to the plane of occurrence of the strip. These stripes cross grain boundaries without changing the orientation of this plane.

When studying the features of formation of shear bands that occur during cold rolling of 316L stainless steel [41], it is shown that these bands are formed in the range of degrees of deformation (70–90%) in grains, which are characterized by layered structures consisting of twin lamellas approximately parallel to the rolling plane. After $\varepsilon \approx 70\%$ deformation, these strips are made up of plates (1 micron long and 0.1

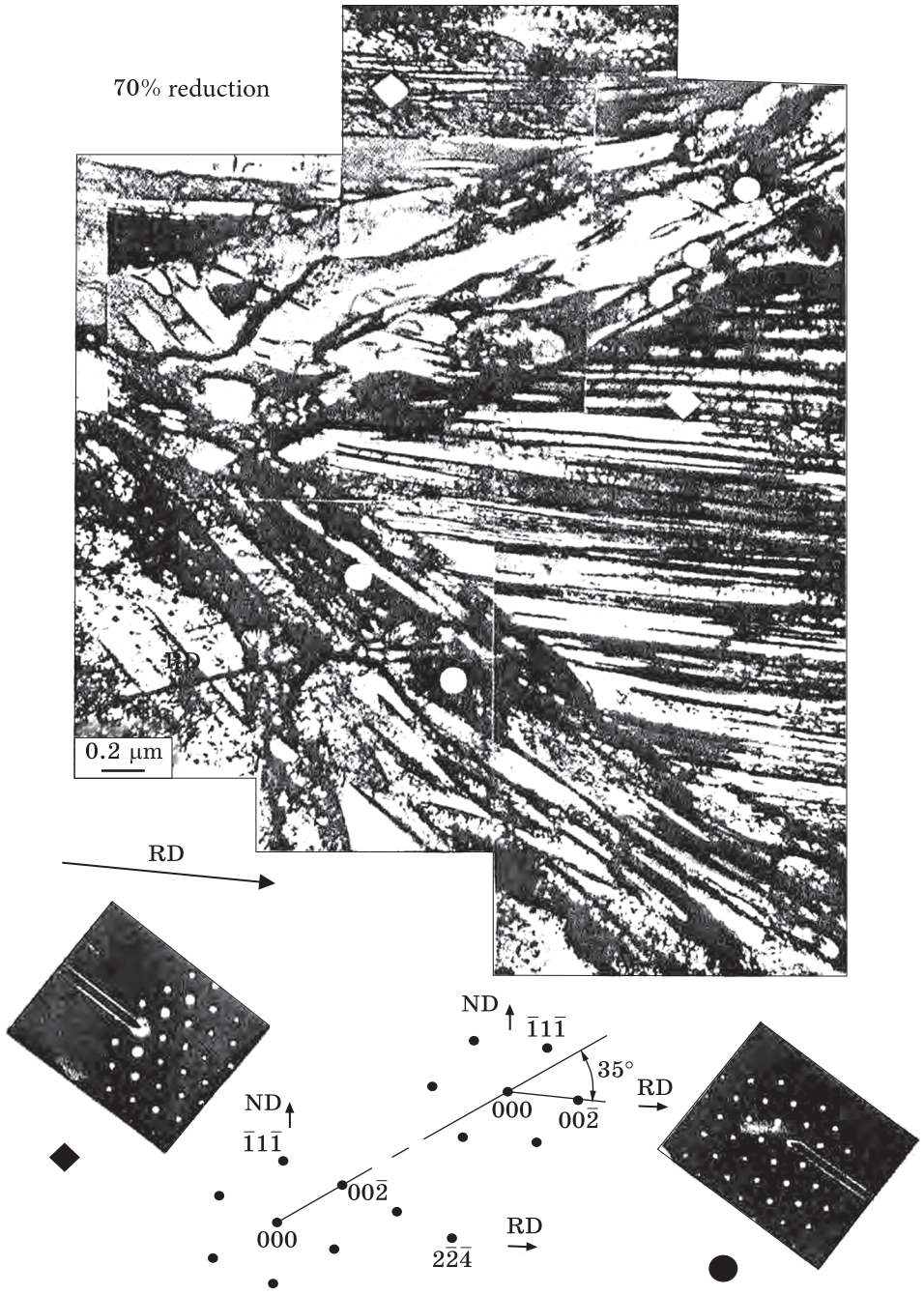

Fig. 2. Localized shift bands in the structure of microdouble circles and rhombuses indicating the orientation of the crystal lattice in the structure of twins and shear bands [41]. ND and RD arrows designate normal and rolling directions, respectively

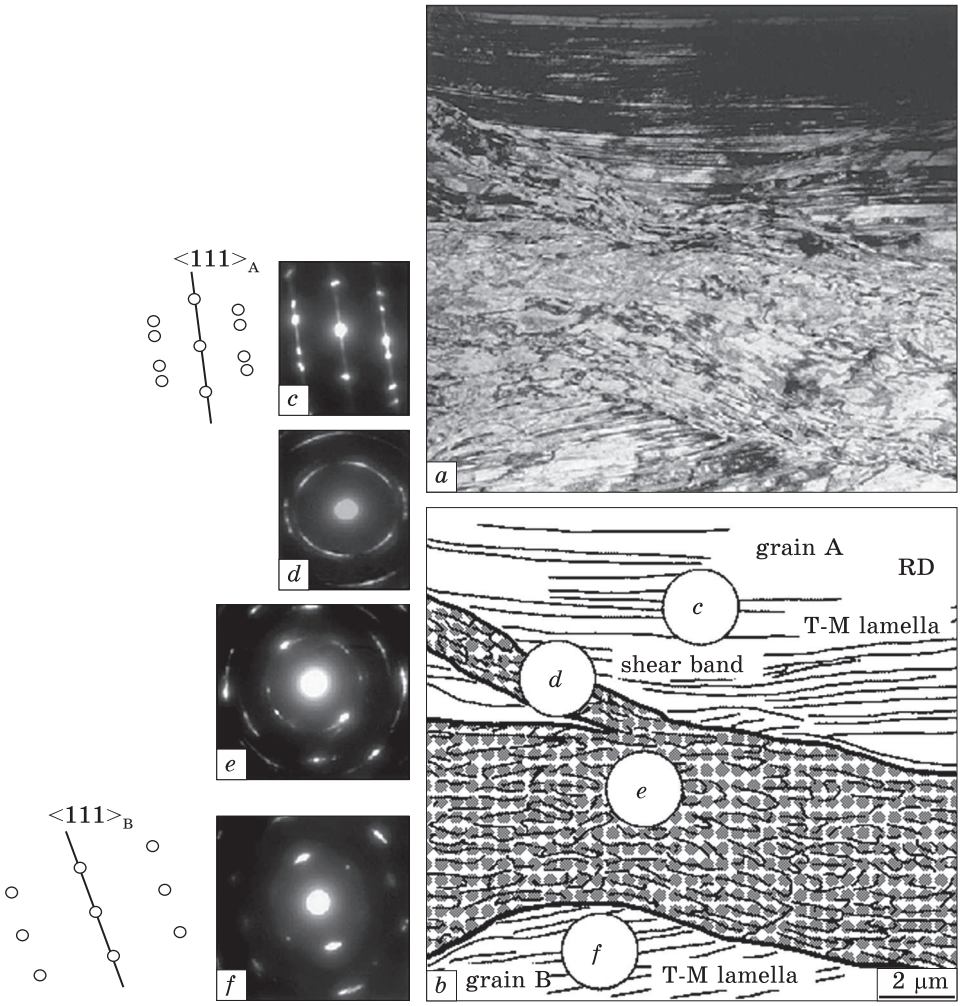

Fig. 3. Features of the shear band microstructure in AISI-201 steel after plastic deformation of 70%, where *a* is a light-field image, *b* is a microstructure diagram, and *c*–*f* are the microdiffraction patterns from the corresponding sections [42]

micron wide) that have been elongated in the direction of shear. With a degree of deformation of 90 %, they are divided into equiaxed cells with a size of ≅10 nm. In the longitudinal section of the sample, rhombuses with an internally twinned structure formed by the shear bands of two systems are observed (Fig. 2). The origin of the shear band on strongly curved deformation twins was also observed.

It is assumed that, since the planes {111} initially parallel to the rolling planes rotate by ≈35° in the distorted zone of the crystal, regions favourable for mass sliding in the direction of maximum shear stresses

are formed. Therefore, the shifts penetrate through the twin lamellas. Thus, cells are formed sequentially, elongated along the direction of propagation of the strip. A single strip formed by such shifts initiates further processes of intensive sliding, which leads to the formation of a series of parallel cells elongated in the direction of the shift and subsequently, to the formation of a shift macrostrip [41].

Figure 3 shows an example of electron microscopic analysis of the deformation structure of the shear bands in the vicinity of the grain boundary located along the rolling direction in austenitic steel AISI 201 [42]. The area representing the shear bands includes the initial grain boundary (Fig. 3, *b*). The lower and upper grains are designated *A* and *B*, respectively.

Microdiffraction analysis of different parts of the presented structure reveals different orientations of structural elements. The diffraction patterns show azimuthal blurring of reflexes, indicating the presence of a wide range of disorientations of the crystal lattice in the shear bands region lying between the grains and *A* and *B*. From the analysis of the microdiffraction pattern, it follows that azimuthal misorientation in the band reaches tens of degrees.

As reported in Refs. [43–45], the features of the formation of adiabatic shear bands arising in austenitic steels under dynamic loading states were investigated. The formation of a nanoscale (≅0.1 microns) crystal structure with high-angle (up to 30°) misorientation, the vortex nature of the plastic flow inside the band, dynamic return, dynamic recrystallization, and the formation of an amorphous phase are all observed for specific deformation states (high velocity, large degrees of deformation, adiabatic states). In addition, AISI 304 and AISI-316 (austenitic class) steels are characterized by phase transformations with the formation of α′-martensite. The formation of α′-martensite at the intersection of two systems of twins, as well as twins and the shear bands [our stainless steel] is shown. At the same time, the possibility of increasing the temperature (in times of the order of milliseconds) in the regions of the shear bands to values exceeding the melting point, with rapid cooling with fixation of nonequilibrium states, including the amorphous phase, is noted. The regions [43] adjacent to the shear bands are distinguished, in which accommodative rotations of the crystal lattice for joint deformation of neighbouring grains are observed. The formation of textural components with orientation in the direction perpendicular to the shear direction and in the direction normal to the shear plane is noted. The structure inside the shear bands is also characterized by the formation of a textural component with orientation. The so-called ‘rotational dynamic recrystallization’ has been proposed as a mechanism for the reorientation of the crystal lattice inside the shear bands [43], leading to the formation of nanoscale grains with high-angle

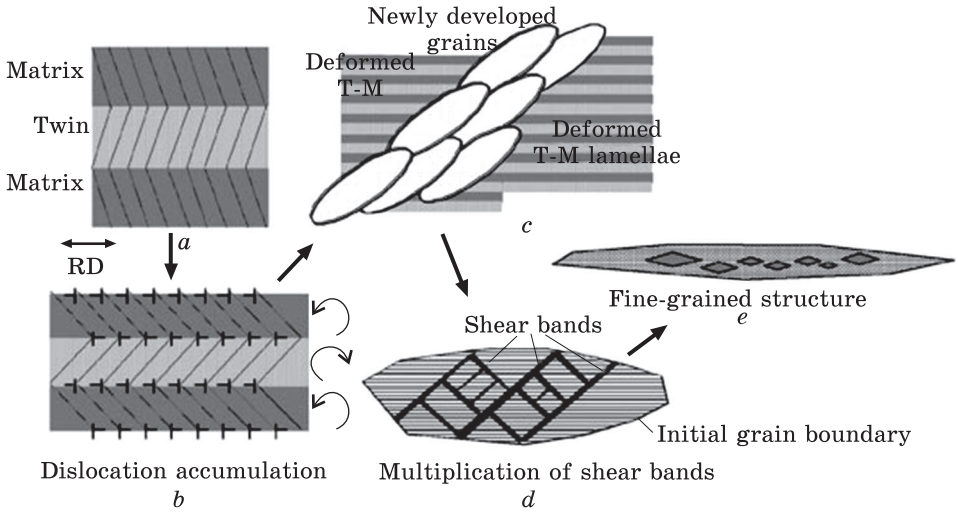

Fig. 4. The process of forming the core of the shear band (*a*, *b*, *c*), multiplication of the shear bands (*d*), and fine-grained structure (*e*) [46]

misorientations. The authors note the difference between this concept and migration dynamic recrystallization.

It was shown in Ref. [46] that, when the shear bands pass through layered structures consisting of twin–matrix (T/M) lamellas, the crystal lattice in the twin rotates clockwise, and in the matrix counterclockwise. This behaviour is explained using the model shown in Fig. 4. With an increase in the degree of deformation during rolling, T/M lamellae become almost parallel to the rolling plane (Fig. 4, *a*), which leads to the activation of sliding in the planes {111} intersecting with the boundaries of the lamellas, both in the matrix and twin regions. Sliding in these planes causes the crystal to rotate clockwise in the twin region and counterclockwise in the matrix region (Fig. 4, *b*). As a result, the orientation of each layer changes, deviating from the original orientation of the double and the matrix. In addition, the activation of sliding leads to the accumulation of a high density of dislocations near the twin boundaries. Locally, dislocations of different signs are annihilated with the formation of new boundaries (Fig. 4, *c*). The annihilation of these boundaries increases the additional sliding, in which the emergence of new boundaries continues. The width of the deformation localization band increases with an increase in the degree of deformation. The T/M lamellar structure collapses with the formation of a fine-grained (nanocrystalline) structure (Fig. 4, *b*). These shear bands increase with increasing deformation during cold rolling, as shown in Fig. 4, *d*. The T/M plate structure must be destroyed to form a fine-grained structure, as shown in Fig. 4, *e*.

In Ref. [47], the evolution of the microstructure after intense shear deformation under adiabatic states of high-speed loading of cold-rolled 316L steel was investigated. It is shown that the substructure in the nascent shear bands consists of elongated lamellar subgrains and fine-crystalline regions. The variation of the substructure from the band boundaries to the centre is represented by the transition from elongated subgrains to rectangular and then to equiaxed subgrains. In the centre, the subgrain bands have an average size of about 80 nm. Rectangular grains are elongated along the shear direction. The combined presence of equiaxed and elongated grains near the centre of the strip suggests that melting is not achieved in the areas of the highest temperature. Small equiaxed grains are formed from elongated subgrains. The destruction and splitting of elongated and rectangular grains is the most likely mechanism for the formation of equiaxed grains. The nucleation and growth of recrystallized grains are poorly expressed due to the limited time of deformation. Deformation-induced and (or) rotational grinding of the structure dominates inside the shear bands. The grain grinding process is controlled by dynamic return at the early stages of strip formation and continuous dynamic recrystallization at the later stages. The evolution of the substructure in the centre of the shear band is characterized by continuous fragmentation. In the process of ongoing localized deformation, small equiaxed subgrains are agglomerated. Clusters of subgrains several times larger than the subgrains themselves experience rotations. Grain boundary sliding and rotations of these clusters become the main mechanism of the developed stage of deformation in the shear band. Deformation twins formed under predeformation states have a significant impact on the development of the shear band. The secondary twins line up along the direction of the shift and lead to the curvature of the primary twins near the band boundary. The sizes of the secondary twins correlate with the initial width of the elongated subgrains. The distance between the primary twins correlates with the initial length of the elongated subgrains in the shear bands. According to the authors of Ref. [47], the mechanism of formation of the fine structure of the deformation localization band is based on the sliding and rotation of clusters containing equiaxed subgrains.

In Ref. [48], the possibilities of using intensive twinning with the formation of high-density twin/matrix lamellas, intersections of the twin matrix lamellar structure over several twinning systems, and deformation localization bands for the formation of nanostructural states in various f.c.c. metals are noted. In Ref. [49], when studying structural transformations occurring in CuZn alloy under states DPD at liquid nitrogen temperature, it was shown that specific deformation states lead to the formation of a high density of deformation twins and nanoparticles in the volume of the material. With an increase in the degree

of deformation in the material, planar dislocation sliding, deformation twinning, and deformation localization bands consistently develop. The thickness of the twins decreases from 48 to 14 nm and reaches saturation at $e > 1.2$. Shear bands occur inside a lamellar structure with a high density of twins with an increase in the degree of deformation. Intense shear deformation is localized inside these bands and leads to the transformation of the twin/matrix lamellas into a nanoscale structure. With a further increase in the degree of deformation, the shear bands widen, which is accompanied by a decrease in the size of the nanograins. The structural state with nanoscale twins and nanosheets demonstrates high values of yield strength (717 MPa) with minimal plasticity (less than 5%). It is assumed that deformation twins play an important role in the hardening of the material, while the formation of shear bands significantly reduces plasticity [49].

The evolution of the microstructure and the mechanisms of the formation of shear bands are studied in detail in Ref. [50] on a Cu–Al alloy under states of DPD. It is shown that the development of the shear band is a two-stage process, represented by the stage of nucleation, leading to the formation of a narrow band consisting of nanoscale subgrains intersecting T/M lamellas and the subsequent stage of expansion of the narrow band due to neighbouring T/M lamellas. The nucleation stage occurs within a narrow region with an almost constant thickness of 100–200 nm, in the so-called 'core' or centre of the strip and consists of three consecutive steps. The first step (1) is initiation of localized deformation (bending, thinning, and bifurcation) in T/M lamellas; the second step (2) is the evolution of the dislocation structure inside the bifurcated strip; and the third step (3) is the transformation of the detwinned dislocation structure (DDS) into a nanosize (sub)grain structure (NGS), Fig. 5. Two transition layers (TRLs) are observed on both sides of the core region of the strip, where T/M lamellas experience much smaller shear deformations.

The surface separating the centre of the strip from the transition layers is characterized by very high gradients of shear deformation, which are accommodated by a high density of dislocations. An increase in shear deformation causes a broadening of the shear band due to its propagation into neighbouring T/M lamellas. At the same time, the broadening occurs by increasing the width of the central part, by the transformation of transition layers (TRLs) into a core containing the DDSs and NGSs, similar to steps (2) and (3) at the origin of the strip. The transition layers are shifted into adjacent T/M lamellas. The grain sizes in a well-developed shear band are larger than the distance between the lamellas in the T/M lamellar structure. A typical structure in which shear deformation with a maximum value of $\gamma_{max} = 2.0$ is localized, as well as areas adjacent to the shear bands and containing a T/M

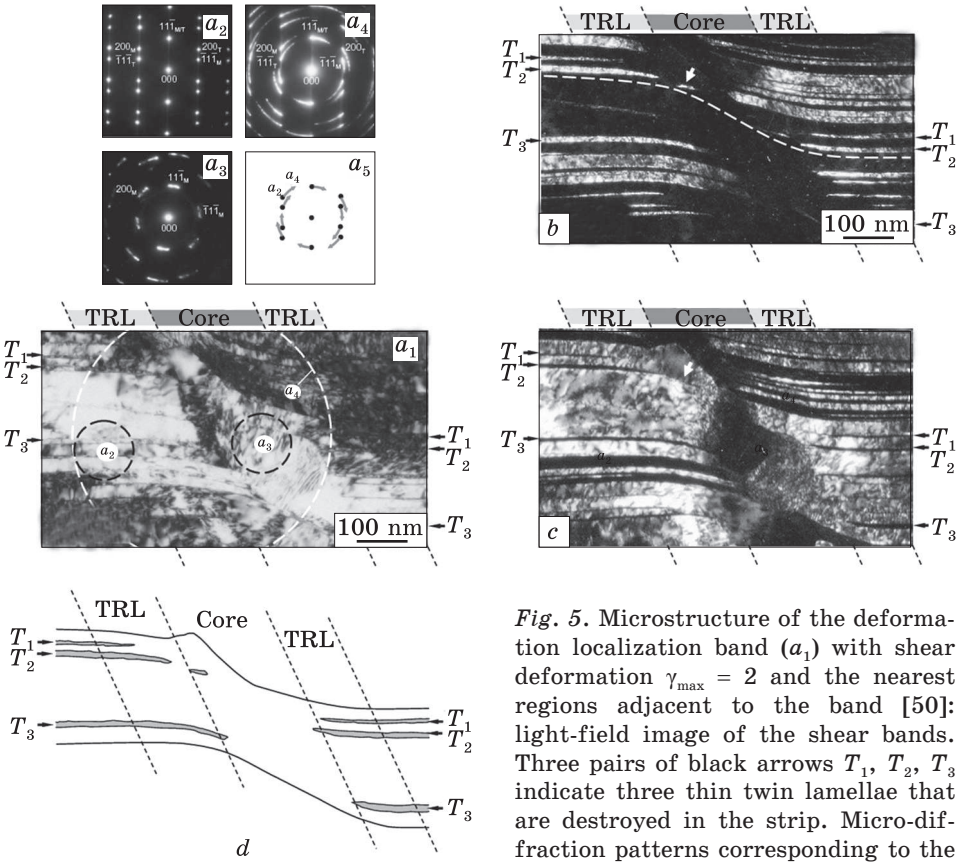

Fig. 5. Microstructure of the deformation localization band (a_1) with shear deformation γ_{max} = 2 and the nearest regions adjacent to the band [50]: light-field image of the shear bands. Three pairs of black arrows T_1, T_2, T_3 indicate three thin twin lamellae that are destroyed in the strip. Micro-diffraction patterns corresponding to the areas marked with circles a_2, a_3, and a_4 on a_1, respectively. Schematic illustration of the relative rotation from a_2 to a_5. Black dots correspond to reflexes on a_2; grey arcs with arrows correspond to reflexes on a_4. Dark-field images revealing twin and matrix lamellae, respectively (*b*, *c*). The white arrow points to the preserved segment of the twin lamella T_2. Schematic illustration of the twins and the shear bands (*d*)

lamellar structure, is shown in Fig. 5 [50]. In the transition layers (TRLs), there is a significant bending of the T/M lamellas. The rotation of the crystal lattice in T/M lamellas and bifurcation inside the shear bands were detected. Fragmentation of the crystal lattice is intensively developing in the core of the strip with the formation of new nanoscale grains (subgrains).

The formation of the shear bands in a layered twin structure (T/M) was observed in single crystals of copper subjected to large plastic deformations of the equal channel angular pressing (ECAP) [23, 51–53]. It is shown that the shear bands are formed in the plane of maximum shear stresses and the orientation of the crystal lattice in them is in a close to twin relation with the matrix. At the same time, a high density

of lamellar twin structures is observed in the matrix according to other twinning systems. The determining role of lamellar structures in the origin of localized shear is noted.

In Ref. [54], the evolution of the microstructure during the formation of nanostructural states under DPD of copper at cryogenic temperatures was investigated [55]. Three mechanisms of plastic deformation and shredding of the structure were found: interaction and redistribution of dislocations, deformation twinning with the formation of nanoscale packages of twin/matrix lamella (T/M lamella), and the development of deformation localization bands in the twin/matrix lamella structure. During the formation of shear bands, T/M lamellas are included in the localized area of the shear band, which is formed at high deformation rates. High degrees of shear deformation can lead to fragmentation and rotation of T/M lamellas, forming elongated or equiaxed crystallites. Ratios close to the twin ones were observed between neighbouring crystallites. For crystallites, which have experienced turns at large angles, the twin ratios are violated. At the same time, secondary twinning within the shear band is not excluded, which becomes possible due to the high deformation rate.

From the above features of the defective structure, the most general patterns of the formation of the shear bands in the micro-twin structure of the twin/matrix can be formulated as follow.

(i) The shear band is formed because of significant bending and a change in the orientation of the twin/matrix lamellae.

(ii) A single formed band leads to further localization of the shift in neighbouring areas and broadening of the shear bands, which develops by bending and fragmentation of the twin/matrix lamellas.

(iii) The shear band has a central part where deformation localization occurs due to crystal lattice reorientation and transition layers with a high density of dislocations and high gradients of shear deformation.

(iv) In the core region of the strip, several (including mutually opposite) processes can be implemented: turns of the crystal lattice (both small-angle and high-angle); grain boundary sliding; secondary twinning; bifurcation (including with successive thinning of primary twins); formation of new grains (subgrains) by dislocation reactions and redistribution of dislocations; dynamic return, dynamic recrystallization, enlargement of new grains. It should be noted the possibility of phase transformations $\gamma \rightarrow \alpha'$ in austenitic steels.

(v) The formation of a nanocrystalline structure is the result of shear band propagation in a micro-double structure. Nanoscale crystallites generally have arbitrary (including high-angle) disorientation of the crystal lattice. At the same time, there is a connection between disorientations in traffic regulations with the twin orientations of the ori-

ginal twin/matrix lamellas and the orientation of secondary twins, or twins of other systems. The bands are characterized by the presence of textural components in the shear plane and the shear direction.

Despite the significant commonality of the processes of formation of adiabatic shear bands under states of dynamic deformations and shear bands formed under states of large deformations by traditional methods with a lower deformation rate (rolling, all-round forging, ECAP, torsion under pressure, *etc.*), it should be noted that much more stringent states for the formation of the shear bands in the adiabatic case. Therefore, not all the regularities of the formation of adiabatic shear bands are directly applicable to 'normal' states of large plastic deformations, in which the deformation rate is less by one or several orders of magnitude and the removal of thermal energy released during deformation is realized.

A number of mechanisms for the formation of deformation localization bands have been proposed, but in many cases, these mechanisms are unable to describe satisfactorily the observed patterns. The latter fully applies to the bands of localization of deformation with the reorientation of the crystal lattice at large (tens of degrees) angles with the presence of a discrete spectrum of selected disorientations: $\approx 35°$, $\approx 50°$ and $\approx 60°$ around the directions. Such disorientations of the crystal lattice cannot be described within the framework of traditional dislocation deformation mechanisms, which is primarily due to the collective (cooperative) nature of their formation. Nevertheless, most of the currently discussed mechanisms for the formation of the shear bands are based precisely on the dislocation mechanisms of plastic flow. The involvement of ideas about partial disclinations or their dipoles as collective carriers of the rotational mode of deformation [56, 57] also cannot explain the high-angle nature of the lattice reorientation in the shear bands with the existence of preferential disorientation vectors, or selected textural directions. Special attention should be paid to the issue of phase instability of the crystal during the formation of high-strength nanostructural states in the bands of deformation localization in austenitic steels. Largely, this situation is due to the lack of experimental studies of the shear bands with a discrete high-angle character of the reorientation of the crystal lattice. In particular, such issues as crystallogeometric patterns of reorientation, subtle features of their internal defective substructure, *etc.* In this situation, it is necessary to conduct experimental studies of the above-mentioned features and develop new physical approaches and mechanisms of deformation, taking into account the phase instability of the crystal in the fields of high local stresses realized in the regions of the deformation localization bands. The original studies presented below on the microstructure features of deformation localization bands in stable austenitic steels are devoted to solving the above problem.

3. Evolution of Microstructure during Rolling

Electron microscopic studies have shown that a sufficiently high density of crystal structure defects is observed in highly nitrogenous steels already in the hardened state. In addition to the chaotic quasi-homogeneous distribution of rectilinear and curved dislocations and dislocation clusters, there are areas containing micro-twins and (or) thin plates of the ε-phase. Apparently, the formation of this defective structure occurs because of high local internal stresses arising during the quenching process.

Steels exhibit intense mechanical twinning beginning with a deformation of $\varepsilon = 10\%$. In the range $\varepsilon = 10–50\%$, mechanical twinning is the dominant mode of deformation. At the same time, the twins, forming in favourably oriented grains, tend to turn in the process of deformation into a plane parallel to the rolling plane. Therefore, at $\varepsilon \geq 30\%$, the plates of microdoubles are practically parallel or form small angles with the rolling plane. When electron microscopic examination of thin foils in sections parallel to the rolling plane, their detection (especially in cases when the twin reflexes on the electronograms coincide with the matrix ones) without special techniques of electron microscopic analysis is often impossible [58].

The first shear bands appear in high-nitrogen steels at $\varepsilon \approx 30\%$. With a further increase in the degree of deformation, when the double mode of deformation is completely exhausted, their formation becomes the main mechanism of plastic shaping during rolling [58]. The density of the strips in the volume of the material increases with deformation. Inside the bands, the crystal lattice fragments into a nanostructured state. The intensity of fragmentation increases with an increasing degree of deformation. The intersection of bands with an internal fragmented structure with micro-twins and bands of different directions with each other leads to the formation of a nanocrystalline state in significant volumes of the material. The structural state with high continuous disorientations formed prior to the formation of the shear bands is critical for further investigation. This state is a characteristic feature of defective substructures of metallic materials after large plastic deformations.

The above results allow us to identify the following. On our opinion, the most important states for the formation of the shear bands in the considered high-nitrogen steels are:

- complete exhaustion of the plastic deformation resource by the mechanisms of dislocation sliding and mechanical twinning;
- intensive deformation hardening during the formation of deformation microdoubles and highly-defective structural states with high curvature of the crystal lattice;
- the presence of high local internal stresses.

The further evolution of the defective structure is developed by fragmentation of the crystal lattice during the propagation of high-angle disorientations in the structure, containing packages of micro-twins in several twinning systems.

4. Evolution of Microstructure under Large Plastic Deformations

According to the results presented above, under rolling states of stable austenitic steels (both high-nitrogen and chromium–nickel ones), the formation of α′-martensite was not detected. However, in the papers [59–61] with large plastic deformations of austenitic steel of the AISI-316 type, the formation of a certain amount of martensitic phase is shown. The 316-type steels have sufficiently high phase stability and do not experience $\gamma \rightarrow \alpha'$ martensitic transformations during processing: forming, rolling, cold drawing, *etc.* In this regard, additional studies were carried out on changes in the phase composition and evolution of the defective structure in a wide ($e \approx 0.3$–6) range of degrees of deformation by rolling and torsion under pressure of AISI-316 steel. In the process of studying the phase composition by x-ray diffraction analysis, no phases were found, except for the initial austenite, in the entire range of the studied degrees of deformation. Electron microscopic studies have shown that, under states of rolling deformation $\varepsilon \leq 50$ % ($e \leq 0.7$), along with deformation twins, the formation of ε-martensite is observed. These are plates with a thickness of a few tenths of a micron and a length of one micron, which are quite rare. At deformation values of $\varepsilon \geq 70$ % ($e \geq 1$), under states of formation of bands of localization of deformation and destruction of the twin structure, the ε-phase is not detected. The formation of a b.c.c. phase with a lattice parameter a = = 2.86 Å, characteristic of α (α′)-martensite, was detected at $\varepsilon \geq 70$ % ($e \geq 1$). Whereas the above phases are not detected by x-ray diffraction analysis methods, their volume fraction does not exceed ≈1%. Based on electron microscopic studies, two types of particles with a b.c.c. lattice can be distinguished, significantly differing in size and distribution pattern. The first type of particles are thin plates with a length of circa 1 micron or a few more and a width of a few tenths of a micron, which are found in the zones of microtwin deformation and inside the shear bands. According to morphology and characteristic sizes, these particles can be attributed to α′-martensite.

An example of a dark-field image of a microstructure in the active reflection of austenite inside the formed shear bands is shown in Fig. 6 [62]. Electron microscopic analysis has shown that this band has a fragmented structure with a predominance of fragments with high-angle misorientations close to 60° and 35°. As can be seen from Fig. 6, *b*, reflexes of α′-martensite are observed on the microdiffraction pattern with

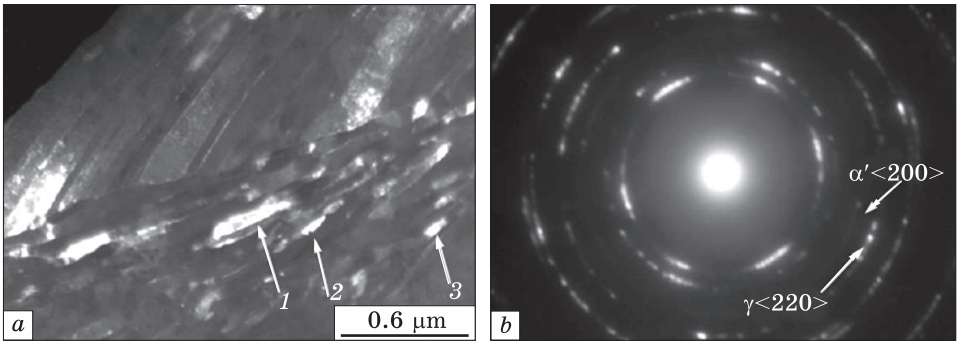

Fig. 6. A local deformation band after rolling to ε ≈ 70% (*e* ≈ 4.6): *a* — dark field image in the reflection *g* = ⟨220⟩ of the γ phase; *b* — selected-area electron diffraction (SAED) pattern [62]

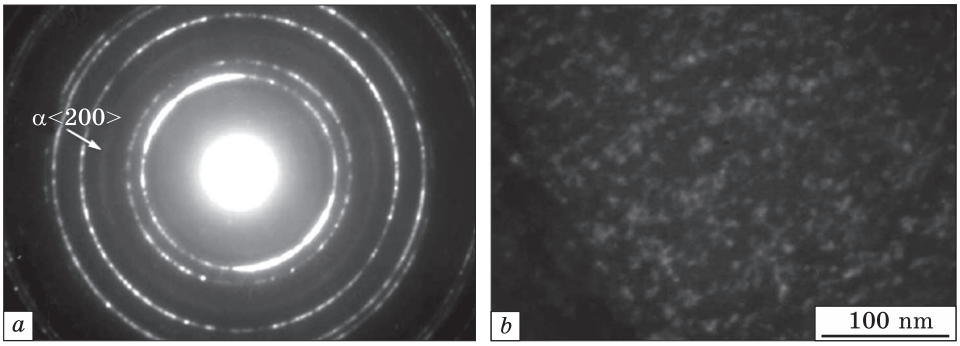

Fig. 7. Nanosized particles of the α phase in the austenitic steel after deformation by high-pressure torsion (HPT) to *e* ≈ 6: *a* — SAED pattern; *b* — dark-field image in the reflection *g* = ⟨200⟩ of the α phase [62]

the shear bands. Dark-field analysis showed that particles of this phase are observed inside fragments of ≈60° reorientation of austenite. Examples of such fragments are shown in Fig. 6, *a* by arrows. Consequently, the formation of these fragments involves the process of deformation γ→α′-transformation in the bands of deformation localization.

After ε ≈ 95–99 % rolling deformation of the plate particles, the α′ phase was not detected. Consequently, in the process of ongoing (after ε ≈ 70 %) plastic deformation, these particles are transformed into the austenitic phase (α′→γ-transformation). A similar sequence of phase transformations is observed in the process of deformation on Bridgman anvils. At *N* = 1 (*e* ≈ 3.8–4.3), as well as after rolling at deformation values *e* > 1, plates of α′-martensite are detected. There are no such plates at *N* = 5 (*e* ≈ 5.5–6),

Particles of the b.c.c. phase of the second type were detected throughout the studied range of large degrees of deformation (*e* ≥ 1) by

rolling and torsion under pressure. They are fine-dispersed secretions (Fig. 7) with a size of <10 nm [62]. In contrast to the lamellar secretions of α′-martensite, these particles will be further designated as the α-phase. Diffraction maxima from such particles (shown by the arrow in Fig. 7, *a*), compared with the diffraction maxima obtained from α′-martensite particles, are much weaker and blurred in the azimuthal direction. As can be seen from the dark-field image obtained in the α-phase reflex ⟨200⟩ (Fig. 7, *b*), their sizes in the entire studied interval $e \approx 1–6$ are in the range from ≈3 to ≈10 nm. At a maximum value of $e \approx 6$ (after torsion under pressure at $N = 5$), the diffraction maxima from these particles give an almost annular electronogram (Fig. 7, *a*).

At $\varepsilon \approx 70$ % ($e \approx 1.2$), signs of a magnetically ordered phase appear. A feature of the magnetization curves is the abnormally large values of magnetic susceptibility in the region of large (up to 10 kE) magnetizing fields. The latter is characteristic of superparamagnets, *i.e.*, local ferromagnetic regions of small size in a paramagnetic matrix, which do not interact with each other. Comparison of these results with the above data of electron microscopic examination indicates that these regions are alpha-phase particles with sizes less than 10 nm.

The particles of the above-mentioned superparamagnetic α-phase must be evenly distributed across the volume of the material, both in the zones of the deformation microarrays and inside the deformation localization bands, in order to analyse the reasons for their formation. In contrast to the plates of α′-martensite (Fig. 6), no connection of these particles with fragments of disorientation or microarrays of deformation was found. In contrast to the plates of α′-martensite (Fig. 6), no connection of these particles with fragments of disorientation or microarrays of deformation was found.

A phenomenon of superparamagnetism similar to the one presented above was found in Refs. [63–65]. In Ref. [63], it was observed after deformation ($\psi = 28$ %) of 18Cr–N–21Mn steel at liquid nitrogen temperature, and, in Ref. [64], after large ($\varepsilon \approx 86$ %) plastic deformations of 12Cr–30Ni and 12Cr–30Ni–Ti steels at room temperature. In Ref. [63], this phenomenon is associated with the formation of finely dispersed (≈20 nm) particles of deformation martensite by the mechanism of $\gamma \rightarrow \varepsilon \rightarrow \alpha'$-transformation, and in Ref. [64, 65], with dispersed clusters of ferromagnetic γ-component. It is assumed [64, 65] that their formation is the result of the redistribution of alloying elements initiated by flows of point defects of deformation origin. It was shown in Ref. [65] that, in steels 12Cr–30Ni and 12Cr–40Ni, the enrichment of effluents with nickel is most likely due to the substitution of mainly iron atoms. At the same time, the concentration of nickel on the drains of point defects can increase from 30 to 40–50 at.% in steel 12Cr–30Ni and from 40 to more than 50 at.% in steel 12Cr–40Ni.

On the other hand, according to the Fe–Ni–Cr system state diagram, in the steel studied here with a chromium concentration of 17 at.% for the formation of local alpha-phase zones, it is enough to deplete them with Ni by only a few (from 14 to 10–12) atomic percent. With the very high effluent efficiency of point defects indicated above (for steels 12Cr–30Ni and 12Cr–40Ni [65]), the probability of formation of such zones with subsequent $\gamma \rightarrow \alpha$ transformation is very high.

According to Refs. [64, 65], the deformation-initiated stratification of a solid solution discussed here is a consequence of a high concentration of deformation point defects with large plastic deformations, leading to an increase in the diffusion rate by several orders of magnitude. The point defects generated in the process of plastic deformation move to the sources (dislocations and other structural defects). A counter flow of alloying elements arises towards the vacancy flows, migrating at different speeds and leading to the formation of local zones enriched or depleted by these elements.

Analysing the above processes in relation to the results of this work, the features of the elastic-stressed state of the material are important. The formation of specific high-defect states with high curvature of the crystal lattice under large plastic deformations determines a high level of local internal stresses, as well as, no less importantly, high stress gradients. Note, in this regard, two important circumstances.

Firstly, the gradients mentioned above are capable of providing both intense flows of deformation point defects [66, 67] (including vacancies as in $\alpha' \rightarrow \alpha''$-martensite [68–70]) and upward diffusion of alloying elements (effects of cyclic martensitic $\gamma–\varepsilon$ and $\gamma–\varepsilon–\gamma$ transformations on diffusion characteristics (of cobalt and carbon) in iron–magnesium-based alloys are reported in Refs. [71, 72]). Simultaneously, local zones of high internal stresses can act as effective sinks of vacancies or interstitial atoms with elastic deformation of the crystal lattice reaching $\varepsilon_{\text{elastic}} = \Delta d/d \approx 2–3$ % (where d is an interplane distance).

Secondly, a high level of local stress can not only stimulate the processes of solid-solution stratification but also change the thermodynamic states of phase transformations, *i.e.*, reducing, *e.g.*, the level of stability of austenite or the barrier of alpha-phase nucleation.

Thus, the above results indicate the possibility of implementing two types of $\gamma \rightarrow \alpha(\alpha')$ transformations in the studied austenitic steel with large plastic deformations.

• The $\gamma \rightarrow \alpha'$ transformation is a transformation leading to the formation of deformation α'-martensite plates closely related to the elements of the defective substructure. At the same time, an increase in the degree of deformation leads to the reverse ($\alpha' \rightarrow \gamma$) transformation of these plates into austenite. An important feature of this transformation is that the α'-martensite formed in this case is an unstable (metastable)

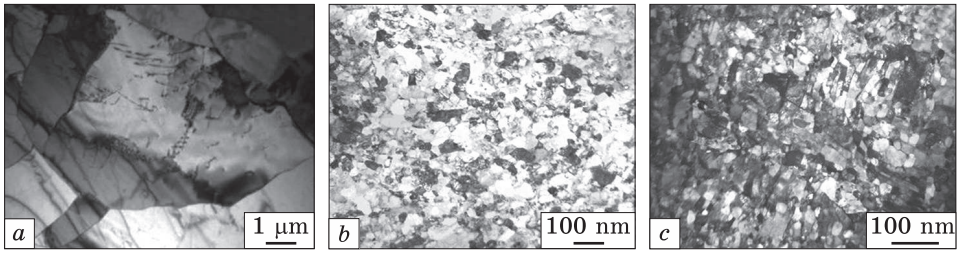

Fig. 8. Microstructure of AISI-316 steel in the initial state (*a*), after 8 passes of HPT at 20 °C (*b*), and after 8 passes of HPT at –196 °C (*c*) [73]

phase that exists either directly during deformation or in the form of thin plates of submicron sizes stabilized by high local residual stresses of highly defective deformation substructures.

• The γ→α-transformation with the formation of nanoparticles of a superparamagnetic b.c.c. (α) phase with dimensions less than 10 nm, the volume content of which continuously increases with an increasing degree of deformation.

Also in Refs. [73–75], a comparison of the evolution of the microstructure and phase transformations of AISI-316 steel that occur during high-pressure torsion at room and cryogenic temperatures was made. As shown in Fig. 8, *a*, the structure of metastable austenitic steel AISI-316 in its initial state contains ≈100 % austenite, polyhedral grains with thin boundaries and annealing twins. The initial state was obtained by quenching.

Eight cycles of deformation by the high-pressure torsion method at room temperature lead to the formation of an equiaxial homogeneous microstructure of 50–60 nm in size, consisting of a mixture of austenite and α-martensite (Fig. 8, *b*). The formation of the nanostructured state occurs due to the action of two mechanisms. The first mechanism is associated with the fragmentation of the initial grains due to the formation of shear deformation bands and twins of deformation origin, and the second mechanism is associated with the development of the phase transformation γ→α by the shear mechanism of formation of deformation martensite. The results of the reduction processes are observed in the structure since the grains are equiaxed with clearly visible boundaries [74].

The structure obtained after 8 high-pressure torsion passes under cryogenic deformation (Fig. 8, *c*) is identical to the structure obtained after deformation at room temperature. However, under cryogenic states, grains are crushed more intensively to 30–40 nm that can be explained by a very high density of defects and grain boundaries that inhibit the movement of particles of dislocation and slow down grain growth. Therefore, the resulting structure is more homogeneous.

A comparison of the microstructure obtained at deformation after ambient temperature and cryogenic temperature showed that up to 4 deformation cycles, the grain size practically does not depend on the deformation temperature and only after 5 passes begins to decrease more intensively when nitrogen is used. This is due to the presence of more barriers introduced during cryodeformation, which prevent dislocations from moving. Liquid nitrogen cooling also contributed to the effective suppression of dynamic recovery processes during deformation, which led to a significantly higher density of defects and, consequently, increased strength properties [73].

5. Conclusions

This article reviews, analyses, and summarizes the results of publications classically based on the theory of dislocations and modern models of strength and plasticity from the positions of various hierarchical levels of localization of plastic deformation.

Despite the half-century history of studying the phenomenon of localization and an impressive number of both theoretical and experimental papers on this problem, the phenomenon of the origin and growth of shear bands remains an insufficiently studied phenomenon, leaving many unresolved issues. This is largely due to the large variety of processes and phenomena accompanying severe plastic deformation, as well as the complexity of experimental observations of the development of the microstructure of the material at high deformation rates. In addition, the development of computer modelling methods and molecular dynamics studies only in recent decades has allowed us to begin a quantitative study of the localization problem from the perspective of the development of defective substructures, which are always present in real materials. This gave a new impetus to research into the causes of localization and opened prospects for a comprehensive understanding of this problem. Meanwhile, new areas available for research have also appeared, such as the study of localization in nanocrystalline metals or metallic glasses. All of the above shows the relevance of further comprehensive studies of the localization phenomenon.

REFERENCES

1. L.B. Zuev, *Annalen der Physik*, **513**, Nos. 11–12: 965 (2001); https://doi.org/10.1002/andp.200151311-1205
2. G.G. Kurapov, E.P. Orlova, I.E. Volokitina, and A. Turdaliev, *J. Chem. Technol. Metall.*, **51**: 451 (2016).
3. A. Naizabekov and I. Volokitina, *Metallurgist*, **64**: 1029 (2021); https://doi.org/10.1007/s11015-021-01083-3
4. R.Z. Valiev, *Nature*, **419**: 887 (2003); https://doi.org/10.1038/419887a

5. P.J. Wray, *J. Appl. Phys.*, **41**: 3347 (1970); https://doi.org/10.1063/1.1659423
6. A.A. Presnyakov, *Lokalizaciya Plasticheskoy Deformatsii* [Localization of Plastic Deformation] (Moscow: Mechanical Engineering: 1983) (in Russian).
7. A.A. Presnyakov, *Ischeznovenie Defektov Upakovki pri Plasticheskoy Deformatsii Polikristallov* [Disappearance of Packaging Defects at a Plastic Deformation of Polycrystals] (Solid State Physics: 1975) (in Russian).
8. Z. Horita, D.J. Smith, M. Furukawa, M. Nemoto, R.Z. Valiev, and T.G. Langdon, *J. Mater. Res.*, **11**: 1880 (1996). https://doi.org/10.1557/jmr.1996.0239
9. S.M. Walley, *Metall. Mater. Trans. A*, **38**: 2629 (2007); https://doi.org/10.1007/s11661-007-9271-x
10. *Adiabatic Shearing in Metallurgical Applications of Shock-Wave and High-Strain-Rate Phenomena* (Eds. L.E. Murr, K.P. Staudhammer, and M.A. Meyers) (New York and Basel: Marcel Dekker Inc.: 1986).
11. T.W. Wright, *The Physics and Mathematics of Adiabatic Shear Bands* (Cambridge: Cambridge University Press: 2002).
12. Y. Xu, J. Zhang, Y. Bai, and M.A. Meyers, *Metall. Mater. Trans. A*, **39**: 811 (2008); https://doi.org/10.1007/s11661-007-9431-z
13. H. Tresca, *Proc. Inst. Mechanical Engineers*, **30**: 301 (1878).
14. W. Johnson, G.L. Baraya, and R.A.C. Slater, *Int. J. Mech. Sci.*, **6**: 409 (1964); https://doi.org/10.1016/S0020-7403(64)80001-1
15. C. Zener and J.H. Hollomon, *J. Appl. Phys.*, **15**: 22 (1944) https://doi.org/10.1063/1.1707363
16. A. Volokitin, A. Naizabekov, and S. Lezhnev, Research of a new method of deformation — pressing–drawing on mechanical properties of steel wire, *Proc. of the Metal 2013 — 22nd Int. Conf. on Metallurgy and Materials (15–17 May 2013)* (Brno: 2013); p. 376.
17. A.L. Wingrove and G.L. Wulf, *J. Australia Inst. Metals*, **18**: 167 (1973).
18. L.S. Magness, *Mech. Mater.*, **17**: 147 (1994); https://doi.org/10.1016/0167-6636(94)90055-8
19. M.L. Wilkins, *Int. J. Eng. Sci.*, **16**: 793 (1978); https://doi.org/10.1016/0020-7225(78)90066-6
20. A.V. Volokitin, K.A. Kambarov, and M.A. Latypova, *Metal Sci. Heat Treatment*, **63**: 341 (2021); https://doi.org/10.1007/s11041-021-00692-8
21. D. Rittel and Z.G. Wang, *Mech. Mater.*, **40**: 629 (2008); https://doi.org/10.1016/j.mechmat.2008.03.002
22. T. Morikawa, K. Higashida, and T. Sato, *ISIJ International*, **42**: 1527 (2002); https://doi.org/10.2355/isijinternational.42.1527
23. H. Miyamoto, A. Vinogradov, and R. Yoda, *Mater. Trans.*, **50**: 1924 (2009); https://doi.org/10.2320/matertrans.m2009054
24. L. Bracke, K. Verbeken, and J. Penning, *Acta Mater.*, **57**: 1513 (2009); https://doi.org/10.1016/j.actamat.2008.11.036
25. Q. Xue, X. Liao, G. Gray, *Mater. Sci. Eng. A*, **410–411**: 252 (2005); https://doi.org/10.1016/j.msea.2005.08.022
26. G. Xiao, N. Tao, and K. Lu, *Mater. Sci. Eng. A*, **503**: 13 (2009); https://doi.org/10.1016/j.msea.2009.01.022
27. C. Hong, N. Tao, and K. Lu, *Acta Mater.*, **58**: 3103 (2010); https://doi.org/10.1016/j.actamat.2010.01.049

28. D.A. Hughes and N. Hansen, *Acta Mater.*, **48**: 2985 (2000); https://doi.org/10.1016/s1359-6454(00)00082-3
29. Y. Wang, X. Liao, Y. Zhao, E. Lavernia, S. Ringer, Z. Horita, T. Langdon, T. Langdon, and Y. Zhu, *Mater. Sci. Eng. A*, **527**: 4959 (2010); https://doi.org/10.1016/j.msea.2010.04.036
30. I.E. Volokitina, A.V. Volokitin, E.A. Panin, M.A Latypova, and S.S. Kassymov, *Eurasian Phys. Tech. J.*, **19**: 73 (2022).
31. K. Morii, H. Mecking, and Y. Nakayama, *Acta Mater.*, **33**: 379 (1985); https://doi.org/10.1016/0001-6160(85)90080-x
32. F. Basson and J.H. Driver, *Acta Mater.*, **48**: 2101 (2000); https://doi.org/10.1016/s1359-6454(00)00042-2
33. M.C. Mataya, M.J. Carr, and G. Krauss, *Metall. Trans. A*, **15**: 347 (1984); https://doi.org/10.1007/bf02645121
34. B. Hwang, S. Lee, Y.C. Kim, N.J. Kim, and D.H. Shin, *Mater. Sci. Eng. A*, **441**: 308 (2006); https://doi.org/10.1016/j.msea.2006.08.045
35. S. Lezhnev, I. Volokitina, and T. Koinov, *J. Chem. Technol. Metall.*, **49**: 621 (2014).
36. Q. Xue, M.A. Meyers, and V.F. Nesterenko, *Mater. Sci. Eng. A*, **384**: 35 (2004); https://doi.org/10.1016/j.msea.2004.05.069
37. H. J. Yang, J. Zhang, Y.B. Xu, and M. Meyers, *J. Mater. Sci. Technol.*, **24**: 819 (2008).
38. I.E. Volokitina, *Met. Sci. Heat Treat.*, **61**: 234 (2019); https://doi.org/10.1007/s11041-019-00406-1
39. I.E. Volokitina, S.N. Lezhnev, E.P. Orlova, and G.G. Kurapov, *Key Eng. Mater.*, **684**: 346 (2016); https://doi.org/10.4028/www.scientific.net/kem.684.346
40. I.E. Volokitina, *J. Chem. Technol. Metall.*, **55**, No. 2: 479 (2020).
41. C. Donadille, R. Valle, P. Dervin, and R. Penelle, *Acta Metal.*, **37**: 1547 (1989); https://doi.org/10.1016/0001-6160(89)90123-5
42. T. Morikawa, K. Higashida, and T. Sato, *ISIJ International*, **42**: 1527 (2002); https://doi.org/10.2355/isijinternational.42.1527
43. M. Meyers, M. Pérez-Prado, Q. Xue, Y. Xu, and T. Mcnelley, *Acta Mater.*, **51**: 1307 (2003); https://doi.org/10.1016/S1359-6454(02)00526-8
44. I.E. Volokitina, *Metal Sci. Heat Treat.*, **62**, Nos. 3–4: 253 (2020); https://doi.org/10.1007/s11041-020-00544-x
45. H.J. Yang, J. Zhang, Y.B. Xu, and M. Meyers, *J. Mater. Sci. Technol.*, **24**: 819 (2008).
46. K. Higashida and T. Morikawa, SPD structures associated with shear bands in cold-rolled low SFE metals, *Nanomaterials by Severe Plastic Deformation* (Eds. M. Zehetbauer and R.Z. Valiev) (Wiley: 2004); https://doi.org/10.1002/3527602461.ch9f
47. J.B. Hirth and J. Lothe, *Theory of Dislocations* (New York: Wiley: 1982).
48. N.R. Tao and K. Lu, *Scr. Mater.*, **60**: 1039 (2009); https://doi.org/10.1016/j.scriptamat.2009.02.008
49. G.H. Xiao, N.R. Tao, and K. Lu, *Mater. Sci. Eng. A*, **513**: 13 (2009); https://doi.org/10.1016/j.msea.2009.01.022
50. C. Hong, N. Tao, X. Huang, and K. Lu, *Acta Mater.*, **58**: 3103 (2010); https://doi.org/10.1016/j.actamat.2010.01.049
51. A.B. Naizabekov, S.N. Lezhnev, and I.E. Volokitina, *Metal Sci. Heat Treat.*, **57**: 254 (2015); https://doi.org/10.1007/s11041-015-9870-x

52. S. Lezhnev, A. Naizabekov, A. Volokitin, I. Volokitina, E. Panin, and M. Knapinski, *J. Chem. Technol. Metall.*, **52**: 172 (2017).
53. I.E. Volokitina and A.V. Volokitin, *Phys. Metals Metallogr.*, **119**: 917 (2018); https://doi.org/10.1134/S0031918X18090132
54. Y.S. Li, N.R. Tao, and K. Lu, *Acta Mater.*, **56**: 230 (2008); https://doi.org/10.1016/j.actamat.2007.09.020
55. I.E. Volokitina, *Metal Sci. Heat Treat.*, **63**: 163 (2021); https://doi.org/10.1007/s11041-021-00664-y
56. A.E. Romanov, *Solid State Phenom.*, **87**: 47 (2002); https://doi.org/10.4028/www.scientific.net/ssp.87.47
57. M.Yu. Gutkin, A.E. Romanov, and P. Klimanek, *Solid State Phenom.*, **87**: 113 (2002); https://doi.org/10.4028/www.scientific.net/SSP.87.113
58. A.N. Tyumentsev, I.Y. Litovchenko, Y.P. Pinzhin, A.D. Korotaev, S.L. Firsova, and V.A. Nesterenkov, *Novyy Mekhanizm Lokalizatsii Deformatsii v Austenitnykh Stalyakh. Vliyanie Dvoinikovaniya na Zakonomernosti Pereorientatsii Kristallicheskoi Reshetki v Polosakh Lokalizatsii Deformatsii* [A New Mechanism for Localization of Deformation in Austenite Steels. The Effect of Twinning on the Patterns of Reorientation of the Crystal Lattice in the Bands of Deformation Localization], *The Physics of Metals and Metallography* (2003) (in Russian).
59. V. Shrinivas, S.K. Varma, and L.E. Murr, *Metall. Mater. Trans. A*, **26**: 661 (1995); https://doi.org/10.1007/bf02663916
60. H.S. Wang, R.C. Wei, C.Y. Huang, and J.R. Yang, *Phil. Mag.*, **86**: 237 (2006); https://doi.org/10.1080/14786430500254271
61. T. Inamura, K. Takashima, and Y. Higo, *Phil. Mag.*, **83**: 935 (2003); https://doi.org/10.1080/0141861031000065338
62. I.Yu. Litovchenko, A.N. Tyumentsev, N.V. Shevchenko, and A.V. Korznikov, *Phys. Metals Metallogr.*, **112**: 412 (2011); https://doi.org/10.1134/s0031918x11040260
63. A.I. Deryagin, A.I. Uvarov, and V.A. Zavalishin, *Obrazovanie α-Martensita pri Plasticheskoy Deformatsii Austenitnoy Stali 10H18AG21 Povyshennoy Stabil'nosti* [Formation of α-Martensite during Plastic Deformation of Austenitic Steel 10X18AG21 of Increased Stability], *Physics of Metals and Metallography* (1997) (in Russian).
64. V.A. Zavalishin, A.I. Deryagin, and V.V. Sagaradze, *Indutsiruyemoye Kholodnoy Deformatsiey Pereraspredelenie Legiruyushchikh Ehlementov i Izmenenie Magnitnykh Svoistv Stabil'nykh Austenitnykh. Nizkotemperaturnoe Mekhanoindutsirovannoye Atomnoye Rassloenie v Khromonikelevykh Stalyakh* [The Redistribution of Alloying Elements Induced by Cold Deformation and the Change in the Magnetic Properties of Stable Austenitic. Low-Temperature Mechanoinduced Atomic Stratification in Chromium–Nickel Steels], *Physics of Metals and Metallography* (2000) (in Russian).
65. V.M. Bykov, V.A. Likhachev, Yu.A. Nikonov, L.L. Serbina, and L.I. Shibalova, *Fragmentirovanie i Dinamicheskaya Rekristallizatsiya Medi pri Bol'shikh i Ochen' Bol'shikh Plasticheskikh Deformatsiyakh* [Fragmentation and Dynamic Recrystallization of Copper under Large and Very Large Plastic Deformations], *Physics of Metals and Metallography* (1978) (in Russian).
66. V.V. Lizunov, I.M. Zabolotnyy, Ya.V. Vasylyk, I.E. Golentus, and M.V. Ushakov, Integrated diffractometry: achieved progress and new performance capabilities, *Prog. Phys. Met.*, **20**, No. 1: 75 (2019); https://doi.org/10.15407/ufm.20.01.075

67. V.B. Molodkin, H.I. Nizkova, Ye.I. Bogdanov, S.I. Olikhovskii, S.V. Dmitriev, M.G. Tolmachev, V.V. Lizunov, Ya.V. Vasylyk, A.G. Karpov, and O.G. Voytok, The physical nature and new capabilities of use of effects of asymmetry of azimuthal dependence of total integrated intensity of dynamical diffraction for diagnostics of crystals with the disturbed surface layer and defects, *Usp. Fiz. Met.*, **18**, No. 2: 177 (2017);
https://doi.org/10.15407/ufm.18.02.177
68. T.M. Radchenko, O.S. Gatsenko, V.V. Lizunov, and V.A. Tatarenko, Research trends and statistical-thermodynamic modeling the α″-$Fe_{16}N_2$-based phase for permanent magnets, *Fundamentals of Low-Dimensional Magnets*, (CRC Press: 2022), Ch. 18, p. 343;
https://doi.org/10.1201/9781003197492-18
69. K.H. Levchuk, T.M. Radchenko, and V.A. Tatarenko, High-temperature entropy effects in tetragonality of the ordering interstitial–substitutional solution based on body-centred tetragonal metal, *Metallofiz. Noveishie Tekhnol.*, **43**, No. 1: 1 (2021);
https://doi.org/10.15407/mfint.43.01.0001
70. T.M. Radchenko, O.S. Gatsenko, V.V. Lizunov, and V.A. Tatarenko, Martensitic α″-$Fe_{16}N_2$-type phase of non-stoichiometric composition: current status of research and microscopic statistical-thermodynamic model, *Prog. Phys. Met.*, **21**, No. 4: 580 (2020);
https://doi.org/10.15407/ufm.21.04.580
71. V.Yu. Danilchenko, V.F. Mazanko, O.V. Filatov, and V.E. Iakovlev, Effect of cyclic martensitic γ–ε transformations on diffusion characteristics of cobalt in an iron–manganese alloy, *Prog. Phys. Met.*, **20**, No. 3: 426 (2019);
https://doi.org/10.15407/ufm.20.03.426
72. V.Y. Bondar, V.E. Danilchenko, V.F. Mazanko, O.V. Filatov, and V.E. Iakovlev, Effect of cyclic martensitic γ–ε–γ transformations on diffusion characteristics of carbon in an iron–manganese alloy, *Prog. Phys. Met.*, **19**, No. 1: 70 (2018);
https://doi.org/10.15407/ufm.19.01.070
73. A. Volokitin, A. Naizabekov I. Volokitina, S. Lezhnev, and E. Panin, Thermomechanical treatment of steel using severe plastic deformation and cryogenic cooling, *Mater. Lett.*, **304**: 130598 (2021);
https://doi.org/10.1016/j.matlet.2021.130598
74. A. Volokitin, A. Naizabekov, I. Volokitina, and A. Kolesnikov, *J. Chemical Technology and Metallurgy*, **57**: 809 (2022).
75. A.B. Nayzabekov and I.E. Volokitina, Effect of the initial structural state of Cr–Mo high-temperature steel on mechanical properties after equal-channel angular pressing, *Phys. Metals Metallogr.*, **120**: 177 (2019);
https://doi.org/10.1134/s0031918x19020133

Received 12.08.2022;
in final version, 13.10.2022

М.А. Латипова[1], С.Л. Кузьмін[2], Т.Д. Фєдорова[2], Д.Н. Лаврінюк[2]
[1] Карагандинський індустріальний університет,
просп. Республіки, 30; 101400 Темиртау, Казахстан
[2] Рудненський індустріальний інститут,
вул. 50 років Жовтня, 38; 111500 Рудний, Казахстан

ЛОКАЛІЗАЦІЯ ДЕФОРМАЦІЇ В ПРОЦЕСІ ВЕЛИКИХ ПЛАСТИЧНИХ ДЕФОРМАЦІЙ

Експериментальні дослідження показують, що локалізація пластичної плинності має місце як під час квазистатичної, так і динамічної деформації металів. Вона приводить до утворення виділених областей (ліній, смуг зсуву), у яких величина пластичної деформації та густина дефектів кристалічної ґратниці (дислокацій) у рази перевищують значення цих величин у навколишньому металі. Локалізація є проявом нестійкости пластичної деформації, наслідком того, що у таких областях локалізованої плинности з тієї чи іншої причини пластична деформація відбувається легше, ніж у навколишньому матеріалі. Утворення областей локалізації зменшує міцність зсуву металів; тому даний ефект має враховуватися під час моделювання пружньо-пластичної деформації металів. Крім того, утворення областей з великою густиною дефектів може ініціювати зміну внутрішньої структури металу, наприклад утворення нових міжзеренних меж за інтенсивної пластичної деформації. Тому дослідження механізмів і умов локалізації пластичної плинности є актуальним завданням механіки деформівного твердого тіла та важливе як для чисельного моделювання пружньо-пластичних плинностей у металі, так і з точки зору прогнозування структури та механічних властивостей деформованого металу. Локалізацію пластичної плинности за малих і помірних швидкостей деформації достатньо докладно досліджено у низці робіт. У той самий час немає єдиного розуміння механізмів і специфічних особливостей локалізації пластичної плинности.

Ключові слова: пластична деформація, пластична плинність, мікроструктура, механічні властивості, мартенсит.